



## Semi-Active Control Using MR-Dampers: NCREE Experiences

C. H. Loh<sup>1</sup>, P. Y. Lin<sup>2</sup>

1 Professor, Dept. of Civil Engineering, National Taiwan University, Taipei 10617, Taiwan.  
E-mail: loh0220@ccms.ntu.edu.tw)

2 Research Fellow, National Center for Research on Earthquake Engineering, NARL, Taipei, Taiwan.  
E-mail: pylin@ncree.narl.org.tw

### ABSTRACT

In recent years, many control strategies have been proposed for earthquake and wind hazard mitigation by installing either passive control devices, active control devices, or semi-active control devices. In particular, semi-active control devices have been shown to be quite effective and robust in reducing the structural responses when subjected to strong earthquakes. Because semi-active control devices, such as MR dampers, have the potential to achieve a majority of the performance of fully active systems without requiring the associated large power sources, many applications such as hybrid-base isolation system, is expected to reduce the excessive base drift of the passive-type base isolation. One challenge in the use of semi-active technology is the development of control algorithms that are appropriate for implementation in full-scale structures. A proper selection of control algorithm may be dependent on the available feedback measurements, the number of devices to be implemented, and the type of nonlinearity presented in the semi-active devices and structure. This paper presents the performance evaluation of semi-active control of structure through large-scale experimental studies for earthquake protection during the past few years in NCREE Structural laboratory. Through shaking table tests (in NCREE, Taiwan) the following experiments are investigated: (1) Hybrid-base isolation with MR-damper and fuzzy control, (2) Equipment isolation using MR-dampers: Experimental performance, and (3) Decentralized sliding mode control of a building using MR-damper. Based on the results of shaking table test, the performance of each control algorithm is discussed.

**KEYWORDS:** *Semi-active control, MR-damper, base-isolation system, sliding mode control, , Neuro-Fussy control, LQR control, Smart control device*

### 1. GENERAL INSTRUCTIONS

In recent years Magnetorheological (MR) dampers have been verified with unique ability to create the resisting force following the change of magnetic and fluid field. Due to the sensitivity of MR dampers the dynamic state of the dampers can be generated in milliseconds. Compared to actuators, MR dampers only require low power sources to switch on to the device forces so that no generator was needed to drive the dampers. In past studies, a number of researchers focused on MR dampers modeling in order to describe the behavior more completely and correctly, such as the modified Bouc-Wen hysteresis model (Dyke et al., 1996), the hysteretic bi-viscous model (Wereley et al., 1998). Follow by numerical study the Bouc-Wen model (Wen, 1976) can be versatile to exhibit a wide variety of hysteretic behavior and the Bingham plastic model (Stanway et al., 1987) can also predict the hysteretic behavior effectively. Chang et al. (2000) proposed an inverse neural network (NN) model to approximate the commands of MR dampers. Generally, MR dampers are capable of reproducing the resisting forces easily but inversion from the damper forces to input signal commands is difficult. Besides, for the application of MR dampers to control the structure good control algorithm must also be developed. Yang et al. (1986) proposed new optimal control algorithms for structural control using standard quadratic performance and Riccati equation to generate appropriate force. Under this optimal skill, many theories related to linear quadratic Gaussian (LQG) were demonstrated to produce the optimal force involving  $H_2$  and  $H_\infty$  control algorithms (Limebeer and Anderson, 1994). Another method for minimization of the structural response is sliding mode control algorithm (SMC) (Utkin, 1992 and Moon et al., 2003). Relying on a specific trajectory, this method was designed a converging plane to optimize the control force with external disturbance. In contrast to SMC, fuzzy sliding mode control (Hwang and Lin, 1992) is an intelligent and adaptive method using fuzzy principle in the closed-loop control of nonlinear systems. In this study, various

control algorithms combined with the MR devices is adopted to reduce the seismic response of building structure through experimental studies.

## 2. MR-DAMPER BASED CONTROL SYSTEM

MR-damper is used as the control device in this study. Depends on control objective MR-damper can be installed between the equipment and the floor (for equipment control) or it can be installed within a steel V-brace to transfer the damper force to the first floor of the structure. MR (magnetorheological) damper is a nonlinear device, whose damping coefficient can be changed in real-time. The magnetic field that controls the viscosity of the MR fluid is generated by the application of an electrical current to the coil surrounding the damper chamber. Therefore, higher damping coefficients can be attained by the MR damper simply by increasing the coil current. Since MR damper is a nonlinear device that must be properly modeled before they can be employed within a structural control system. A number of parametric models that fully describe the force-velocity relationships of MR dampers have been formulated [13]. One such parametric model is the Bouc-Wen model, whose computational tractability and model flexibility are attractive features. For the 20 kN MR damper, as an example used in this study, a modified Bouc-Wen model has been proposed (Lin, *et al.* 2005). The force in the MR damper,  $F$ , results from an equivalent viscous damper with the addition of a hysteretic restoring force,  $z$ , is expressed as:

$$F(t) = C(V)\dot{x}(t) + z(t) \quad (1)$$

Here, the damping coefficient,  $C$ , is controllable by the damper command voltage,  $V$ . In this study, the hysteretic restoring force,  $z$ , is defined by a modified Bouc-Wen model [25, 26],

$$\dot{z}(t) = A\dot{x}(t) + \sum_{n=1}^2 a_n \left[ \gamma \dot{x}(t) |z(t)|^n + \beta |\dot{x}(t)| |z(t)|^{n-1} z(t) \right] \quad (2)$$

where,  $A$ ,  $\beta$ ,  $\gamma$  and  $n$  are parametric constants and  $\dot{x}(t)$  is the shaft velocity of the damper. Different from the modified Bouc-Wen model, the modified bi-viscous model and exponential model can also be used to represent the mathematical model of MR-damper (Chang *et al.* 2006).

## 3. DEVELOPMENT OF CONTROL STRATEGIES

Active control has been used against earthquake excitations in both experimental and numerical studies. Various control algorithms such as LQR, LQG, sliding mode control, fuzzy logic control, etc. have been proposed. Each control algorithm has its own feature. In this section some basic control algorithms that were used in NCREE control testing are introduced.

### 3.1. Centralized vs. Fully Decentralized Control

In view of traditional structural control four groups of control algorithms can be discussed: fully centralized control, fully decentralized control, half centralized control, partially decentralized control. Fully centralized control architecture indicated that each actuator (which corresponds to each row of the gain matrix) requires the full state response to determine its control action. Based on the  $H_2$  control algorithms, one can obtain the control force which depends on the full-state vector and the P-matrix (obtained by solving the Riccati equation). Since the full-state cannot be practically acquired in current structural control systems, the Kalman estimator is used to transform the measured output vector of the system into an estimated state vector. The control force can be expressed in following form:

$$\begin{aligned} \mathbf{u}[k+1] &= \mathbf{G}\mathbf{z}_d^{red}[k+1] = \mathbf{G}(\mathbf{A}_d^{red} + \mathbf{B}_d^{red}\mathbf{G} - \mathbf{L}\mathbf{C}_c^{red} - \mathbf{L}\mathbf{F}_d^{red}\mathbf{G})\mathbf{z}_d^{red}[k] + \mathbf{G}\mathbf{L}\mathbf{y}_{d,s}[k] \\ &= \mathbf{G}\hat{\mathbf{A}}_{cs}\hat{\mathbf{z}}_d^{red}[k] + \mathbf{G}\mathbf{L}_{ms}\mathbf{y}_{d,s}[k] \end{aligned} \quad (1)$$

where  $\hat{\mathbf{A}}_{cs}$  is the modified system matrix in relating to the control gain and  $\mathbf{L}_{ms}$  is the Kalman estimator in relating to measurement.

The difference between the fully centralized and the half centralized control is on the coupling effect among control forces. The control gain of each control device of the half centralized control was developed independently. The half centralized control algorithm assumes that each column of  $\mathbf{B}_d^{red}$  to be independent, which means that to obtain the control gain only one location of control devices is considered. Therefore, the

number of objective functions is in corresponding to the number of subsystems as defined. The control force can be calculated as follows:

$$u_i[k] = -(2\hat{R} + (\mathbf{B}_d^{redT})_i \mathbf{P} (\mathbf{B}_d^{red})_i)^{-1} (\mathbf{B}_d^{redT})_i \mathbf{P} \mathbf{A}_d^{red} \mathbf{z}_d^{red}[k] = \mathbf{G}_i \mathbf{z}_d^{red}[k] \quad (2)$$

where  $\mathbf{G}_i$  is a row vector with the same length as the full-state vector, and combine all the control gain to obtain the system control gain (Loh *et al.* 2008)

$$\mathbf{G}_{new} = [\mathbf{G}_1^T, \mathbf{G}_2^T, \dots, \mathbf{G}_n^T]^T \quad (3)$$

The fully decentralized control emphasizes on the control of local system which only the locations of control device and the measurement around the local subsystem are considered. Therefore, a complete structural system can be assumed as composition of many sub-systems and each sub-system contains its own sensor measurements and control devices in that subsystem. For the fully decentralized control it is defined that each controller constitutes a sub-system which is independent and no relation to each other. For the decentralized control the malfunction of individual controller will not cause the failure of the entire control system. Table 1 shows the summarized the control gain and control force for different control algorithm.

Table 1. Summarized the control gain and control force for different control algorithm.

Control Algorithm	Control Gain	Control Force
Centralized control:	$G = [G_{n \times n}]_{16 \times 40}$ , $GL = [GL]_{full, 16 \times 20}$	$u[k]_{16 \times 1} = G z_d^{red}[k]$
Half centralized control	$G = \begin{bmatrix} G_{1,1(1 \times 40)} \\ \vdots \\ G_{i,1(1 \times 40)} \end{bmatrix}_{16 \times 40}$ , $GL = \begin{bmatrix} G_{1,1(1 \times 40)} \\ \vdots \\ G_{i,1(1 \times 40)} \end{bmatrix}_{16 \times 40}$ , $L_{40 \times 20}$	$u[k]_{16 \times 1} = G z_d^{red}[k]$
Fully de-centralized control	$G_i = [G_i]_{1 \times 40}$ $GL_i = G_{i,1 \times 40} L_{i, 40 \times 1}$ , $i = 1 \sim 16$	$u_i[k] = G_i (z_d^{red})_{i, 40 \times 1}[k]$
$\dot{\tilde{z}}[k+1] = (A + BG - LC - LFG)\tilde{z}[k] + Ly[k]$ $u[k+1] = G\tilde{z}[k+1] = G(A + BG - LG - LFG)\tilde{z}[k] + GLy[k]$		

### 3.2. Structural Control Using Decentralized Sliding Mode Control Algorithm

The theory of sliding mode control (SMC) is to design controllers to drive the response trajectory into the sliding surface, whereas the motion on the sliding surface is stable. For linear structures, the r-dimensional sliding surface  $\mathbf{S}=\mathbf{0}$  for r controllers (dampers) can be a linear combination of the state variables, i.e.

$$\mathbf{S} = \mathbf{PZ} = \mathbf{0} \quad (4)$$

where  $\mathbf{S} = [S_1 \ S_2 \ \dots \ S_r]^T$  is a r-vector consisting of r sliding variable, i.e.,

$$\mathbf{P} = [\mathbf{P}_1^T \ \mathbf{P}_2^T \ \dots \ \mathbf{P}_r^T]^T = (r \times 2n) \text{ matrix} \quad (5)$$

and

$$\mathbf{Z} = [z_1 \ z_2 \ \dots \ z_z \ z_{n+1} \ \dots \ z_{2n}]^T = [x_1 \ \dots \ x_n \ \dot{x}_1 \ \dots \ \dot{x}_n]^T \quad (6)$$

$x_i$  is the  $i^{\text{th}}$  inter-story drift,  $n$  is the total number of DOFs,  $\mathbf{P}$  is a  $(r \times 2n)$  matrix to be designed such that the motion on the sliding surface,  $\mathbf{S}=\mathbf{0}$ , is stable, and  $\mathbf{P}_i$  is the  $i^{\text{th}}$  row vector of  $\mathbf{P}$  with a dimension of  $2n$ . Let the  $i^{\text{th}}$  damper be installed in the  $i^{\text{th}}$  story unit and let  $r$  be the total number of dampers in the building. For the decentralized SMC, the  $i^{\text{th}}$  sliding variable  $S_i$  for the  $i^{\text{th}}$  damper is chosen as a function of  $x_{ki}$  and  $\dot{x}_{ki}$ , i.e.,

$$S_i = \alpha_{ki} x_{ki} + \dot{x}_{ki} = 0 \quad (7)$$

where  $\alpha_{ki}$  is the pole of the sliding surface. For the motion to be stable on the sliding surface,  $\alpha_{ki}$  should be positive, i.e.,  $\alpha_{ki} > 0$ . Consequently, it follows from Eqs.(4) and (7) that  $\mathbf{P}_i$ , the  $i^{\text{th}}$  row-vector of  $\mathbf{P}$ , is given by

$$\mathbf{P}_i = [0, 0, \dots, \alpha_{ki}, 0, 0, \dots, 1, 0, 0, \dots, 0] \quad \text{for } i = 1, 2, \dots, r \quad (8)$$

where the elements  $\alpha_{ki}$  and 1 are at the locations of  $ki$  and  $ki+n$ , respectively. Then based on the sliding mode control, the Lyapunov function is expressed as

$$\mathbf{V} = \frac{1}{2} \mathbf{S}^T \mathbf{S} \quad (9)$$

The derivative of the Lyapunov function is obtained:

$$\dot{\mathbf{V}} = \mathbf{S}^T \dot{\mathbf{S}} = \mathbf{S}^T \mathbf{P} \dot{\mathbf{Z}} = \mathbf{S}^T (\mathbf{PB}) [\mathbf{U} + (\mathbf{PB})^{-1} \mathbf{P} (\mathbf{AZ} + \mathbf{E})] \quad (10)$$

Let

$$\boldsymbol{\lambda} = \mathbf{S}^T \mathbf{PB} \quad \text{and} \quad \mathbf{G} = -(\mathbf{PB})^{-1} \mathbf{P} (\mathbf{AZ} + \mathbf{E}) \quad (11)$$

Then, it follows from Eq.(10) that

$$\dot{\mathbf{V}} = \boldsymbol{\lambda} (\mathbf{U} - \mathbf{G}) = \sum_{i=1}^r \lambda_i (u_i - G_i) = \sum_{i=1}^r \lambda_i u_i - \sum_{i=1}^r \lambda_i G_i = \dot{\mathbf{V}}_1 + \dot{\mathbf{V}}_0 \quad (12)$$

where 
$$\dot{V}_1 = \lambda \mathbf{U} = \sum_{i=1}^r \lambda_i \mathbf{u}_i; \quad \dot{V}_0 = -\lambda \mathbf{G} = -\sum_{i=1}^r \lambda_i \mathbf{G}_i \quad (12a)$$

and  $\mathbf{u}_i$  = control force from the  $i^{\text{th}}$  damper. In Eq. (12),  $\lambda_i$  is the  $i^{\text{th}}$  element of  $\lambda^T$  vector (r-vector) and  $\mathbf{G}_i$  is the  $i^{\text{th}}$  element of the r-column vector  $\mathbf{G}$ . Note that  $\dot{V}_0$  is the derivative of the Lyapunov function for the structure without control (i.e.,  $\mathbf{u}_i = 0$ ). Since the structure without control is stable, we have  $\dot{V}_0 \leq 0$ . Therefore, to design the control force, it is necessary to guarantee that  $\dot{V}_1 \leq 0$ .

Two different control strategies will be discussed. First, To design a sliding mode controller for  $\dot{V}_1 \leq 0$ , one possible design is obtained by minimizing  $\dot{V}_1 = \sum_{i=1}^r \lambda_i \mathbf{u}_i$  in Eq. (17). Supposed each story is installed with one damper, i.e.,  $n = r = 6$ . The vector  $\lambda$  in equation (11) can be obtained from  $\lambda = \mathbf{S}^T \mathbf{P} \mathbf{B}$ . Note that the notations defined previously are  $n=6$ ,  $z_i = x_i$  and  $z_{i+6} = \dot{x}_i$ . Further, the row vector  $\lambda$  is different depending on the damper layout. For example, if only one damper was implemented in the first floor, then  $\lambda$  can be determined:  $\lambda = \frac{1}{m_1} (\alpha_1 z_1 + z_7)^T$ . This is defined as the SMC-1. Hence, the minimization of  $\dot{V}_1 = \sum_{i=1}^r \lambda_i \mathbf{u}_i$  depends on the signs of  $\lambda_i$  and  $\mathbf{u}_i$ , and the control law is proposed:

- (1) If  $\lambda_i > 0$  and  $z_{ki+n} > 0$ , then  $\rho_i = \rho_{i \min}$ ; (2) If  $\lambda_i > 0$  and  $z_{ki+n} < 0$ , then  $\rho_i = \rho_{i \max}$ ;
- (3) If  $\lambda_i < 0$  and  $z_{ki+n} > 0$ , then  $\rho_i = \rho_{i \max}$ ; (4) If  $\lambda_i < 0$  and  $z_{ki+n} < 0$ , then  $\rho_i = \rho_{i \min}$ ;

Different from SMC-1, the controller is designed to guarantee that  $\dot{V} = \sum_{i=1}^r \lambda_i (\mathbf{u}_i - \mathbf{G}_i) \leq 0$ . Hence, the control force  $\mathbf{u}_i$  from the  $i^{\text{th}}$  damper (installed in  $i$ -th story) is given by

$$\mathbf{u}_i = \mathbf{G}_i - \delta_i \lambda_i \quad (13)$$

in which  $\delta_i > 0$  is referred to as the sliding margin,  $\mathbf{G}_i$  is the  $i^{\text{th}}$  element of the r-vector  $\mathbf{G}$ , and  $\lambda_i$  is the  $i^{\text{th}}$  element of the r-vector  $\lambda^T$ . One can easily show that  $\dot{V} = \sum \lambda_i (\mathbf{u}_i - \mathbf{G}_i) = -\sum \lambda_i^2 \delta_i \leq 0$ . For the 6-story building structure as an example, the the control force in the 1<sup>st</sup> floor will be

$$\bar{u}_1 = -m_1 (\alpha_1 \dot{x}_1 + (x_1 A_{(7,1)} + \dot{x}_1 A_{(7,7)} - \ddot{X}_0)) - \delta_1 (\alpha_1 x_1 + \dot{x}_1) \frac{1}{m_1} \quad (14)$$

in which  $A_{(i,j)}$  is the  $i$ - $j^{\text{th}}$  element of the system matrix  $A$ . The MR damper installed in the first story requires the measurement of the earthquake ground acceleration  $\ddot{X}_0$  in addition to the responses of the first story. This is defined as the SMC-4 in this study.

### 3.2.1. Decentralized Sliding Mode Control of Building Structure (Lu et al. 2008)

A 1/4-scale 6-story steel frame was designed for this structural control research. As shown in Figure 1, the six-story scale-down structure consists of a single bay with a 1.0 m by 1.5 m floor area and 1.0 m story height. Story height: 1000<sup>mm</sup>, Floor dimension: 100<sup>mm</sup> x 1500<sup>mm</sup>. The identified first five modal frequencies (using

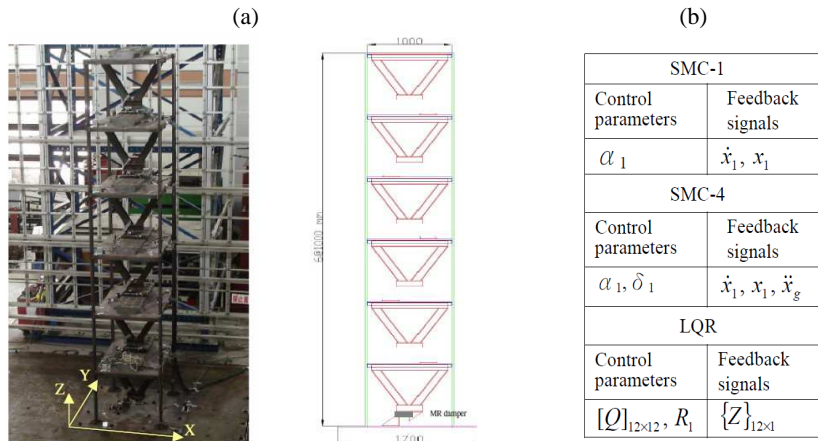


Figure 1. (a) Photo of the 6-story steel structure and the V-shape bracing system is for the installation of damper, (b) Control parameters and feedback signals for SMC-1, SMC-4 and LQR control methods

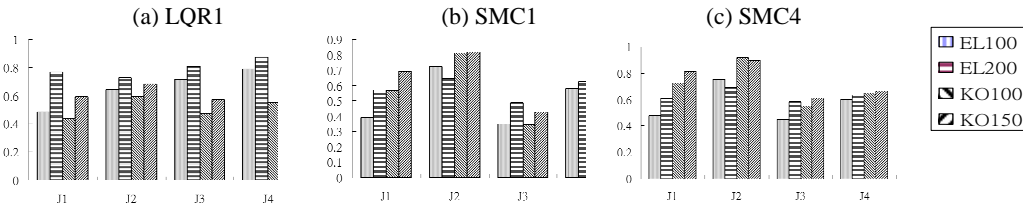


Figure 2. Comparison on performance indices of a test structure subjected to four different earthquake excitations (EL Centro-100gal, and 200gal, Kobe-100gal and 150gal); (a) LQR1 control, (b) SMC1, (c) SMC4

data-driven stochastic subspace identification method (Weng *et al.* 2009) are: 1.05 Hz, 3.50 Hz, 6.12Hz, 8.987 Hz and 11.91 Hz and the corresponding modal damping ratios are: 0.2%, 0.99%, 0.09%, 0.79% and 1.86%. A 3kN MR-damper was used and install in the 1<sup>st</sup> floor. Four earthquake records (EL Centro-100 gal, EL Centro-200 gal, Kobe-100 gal, Kobe-150 gal) are selected as input excitations to examine the effect of different seismic excitations on the performance of various control algorithms. *Figure 2* shows the performance indices of the experimental results for the structure using the passive-on, LQR, SMC-1 and SMC-4 control algorithms. It is observed that, the variances of the performance indices for different ground motions are not significant, and the control performance based on passive-on, LQR, SMC1 and SMC4 control algorithms are plausible.

### 3.2.2. Control performance of semi-active equipment isolation system (Fan *et al.* 2009)

Consider a 3-story steel frame with light equipment located on the first floor. The test structure used in this experiment is designed to be an almost full-scale prototype building and is subjected to a one-dimensional ground motion. The floor dimension is 2 meters by 3 meters and the total height is 9 meters. *Figure 3* shows the schematic diagram of this 3-story model building with the semi-active equipment isolation system on the first floor. In this experiment, a single MR-damper and a frictionless rolling-type isolator are installed between the equipment and the first floor. The friction coefficient  $\mu$  is assumed as 0.0. The MR damper employed here is a 7kN capacity damper with  $\pm 15.0$  cm stroke. The mass of each floor is 6 tons, and the equipment mass is 3 tons. Decentralized sliding mode controller is developed in the test structure with equipment isolation system, as shown in Fig. 3. In this case only one controller, i.e.,  $r \equiv 1$ , and the control vector  $U = u_1$  is a scalar. For full-state sliding mode control, the SMC-4 algorithm to determine the control force can be selected as

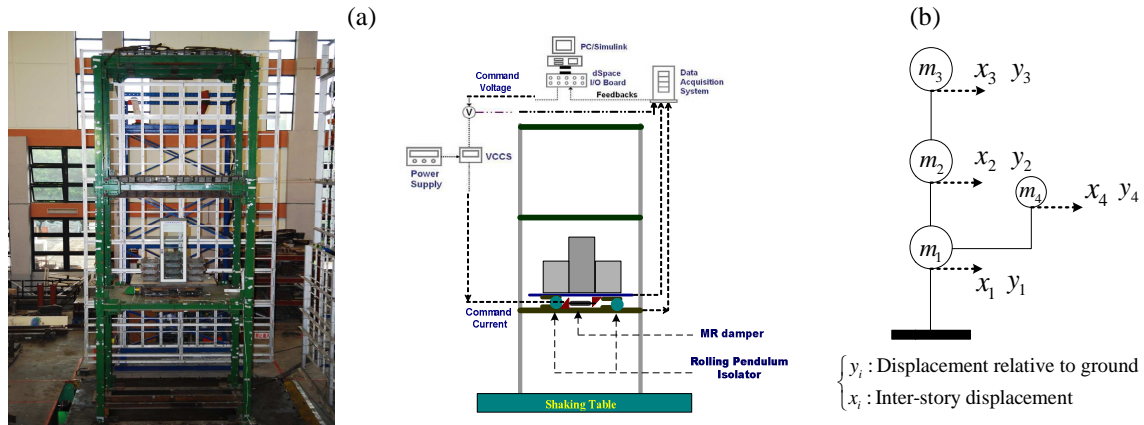


Figure 3. (a) Photo of the test setup and the Schematic diagram of the control test setup. (b) Lumped mass model of a 3-DOF system with equipment on the first floor.

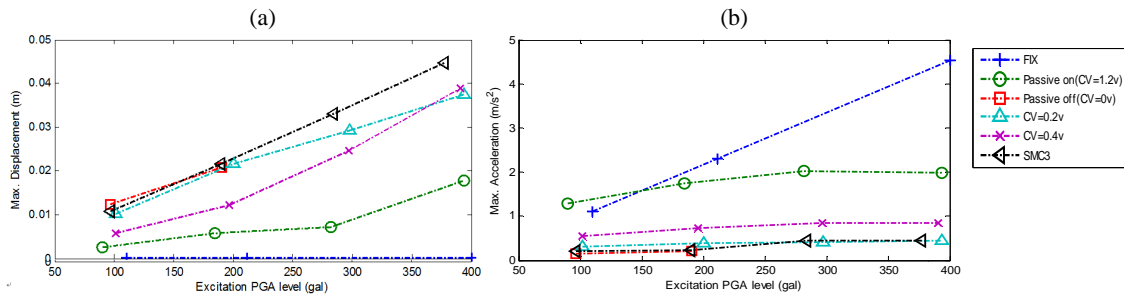


Figure 4. Comparison of the equipa acceleration and the damper stroke among different control algorithms: (the Chi-Chi earthquake data from station TCU129 was used as input motion); (a) plot of maximum relative displacement of equipment w.r.t. excitation level, (b) plot of maximum acceleration of equipment w.r.t. excitation level.

$$u_1 = G_1 - \lambda_1 \delta_1 \quad (15)$$

where  $\bar{G} = m_4 \cdot \mu \cdot \text{sign}(\dot{x}_4) - \alpha m_4 \dot{x}_4 + \beta m_4 \ddot{x}_{1a} + k_4 x_4$  and  $\lambda_1 = (\alpha x_4 + \dot{x}_4) / m_4$  (16)

Then the derivative of the Lyapunov function becomes:  $\dot{V} = -\lambda_1^2 \delta_1 \leq 0$ . In other word, a sliding mode controller can be designed based only on the information obtained at the damper location. . The controller given in Eqs.(15) and (16) is referred to as SMC-4. There are two parameters to be adjusted for the performance of the controller, i.e.,  $\alpha$  and  $\delta$ . Note that the measurement of the ground acceleration  $\ddot{x}_g$  is needed for this controller.

Figure 4 shows the comparisons of the control performance of equipment among different control algorithms: Passive-on (1.2 Volt), Passive-on (0.2 Volt), Passive-on (0.4 Volt), Passive-off, and SMC-4, for different levels of ground excitations.

### 3.3. Control of Hybrid Base Isolation System Using Fussy Control (Lin et al. 2007)

In this study, a base-isolated structure with four high damping rubber bearings (HDRBs) and a 300kN MR damper is tested on a shake table. The goal is to verify effectiveness of the hybrid control system with physical hardware and real-time processing requirements. Figure 5 shows a schematic drawing of the experimental set-up. The isolated structure is constructed with a steel frame and lead blocks that provide a mass of 21,772 kg. Diameter of each HDRB used in the isolation system is 150 mm. Ends of the 300kN MR damper are securely attached to the top surface of the shake table and the bottom of the isolated structure. Design parameters of the damper are listed in Table I. Displacements and accelerations of the base-isolated system are grouped into three levels: base of the HDRB (D0, A0), top of the isolated structure (D1, A1) and top of the isolated structure (D2, A2). The semi-active control device used in this study is a 300kN MR damper. Fuzzy logic is used to map an input space to an output space by means of if-then rules. Use of a fuzzy controller is advantageous in that performance is not overly sensitive to changes in the input signal. Components of the input signal are transformed into linguistic values through a fuzzification interface at each time step. For output the mapped linguistic values are transformed into numerical values through a defuzzification interface.

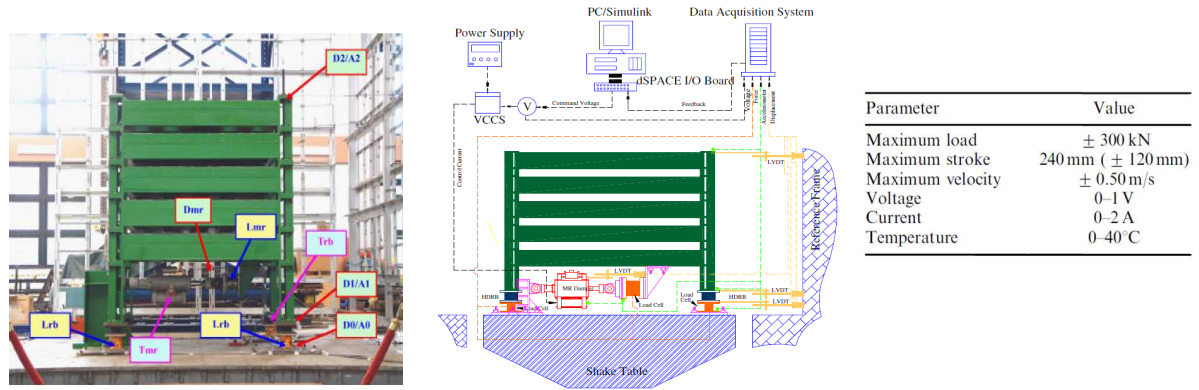


Figure 5. Experimental set-up of test structure and the table shows the operational parameters of 300kN MR damper.

Three proposed candidates for semi-active controllers are used to operate the MR damper during a series of full-scale experiments. For the first controller, S1, the relative displacement and velocity of the isolated mass are selected as input variables while the output of the fuzzy logic controller is the command voltage to the MR damper (see Figure 6a). There are seven triangular membership functions for each input and output variable. Based on numerical simulations, ranges of the relative displacement and velocity are selected to be [0.005, 0.005 m] and [0.1, 0.1 m/s], respectively. When an input is out of range, the boundary value is used. Note that the magnitude of the output command varies from -1.0 to 1.0 V to prevent the undesirable overshooting. For the second controller, S2, the absolute acceleration and relative velocity of the isolated mass are selected as inputs, while the output is the command voltage (see Figure 6b). There are seven membership functions for the first input, absolute acceleration, and also for the voltage output. Five membership functions operate on the second input, relative velocity. The basic design concept for this case is to control the absolute acceleration of the isolated mass through adjustment of force in the damper that is assumed to be proportional to the relative velocity of the mass. Ranges of the absolute acceleration and relative velocity are selected to be [-5, 5 m/s<sup>2</sup>] and [-0.5, 0.5 m/s], respectively. For the third controller, S3, the absolute acceleration and relative displacement of the mass with respect to the base are selected as inputs, and the output is the command voltage (see Figure 6c). The number of membership functions used for the acceleration and displacement inputs are four and six, respectively, while seven membership functions are used for the output. The design approach for this case is to

control both the absolute acceleration and the relative displacement of the isolated mass. For this controller ranges of the absolute acceleration and relative displacement are selected to be  $[-5, 5 \text{ m/s}^2]$  and  $[-0.005, 0.005 \text{ m}]$ , respectively.

Effectiveness of each control scheme can be determined from data collected during testing on the shake table. Data are presented according to maximum response under different level of base excitation (El Cento earthquake). In order to facilitate comparison of results from a large number of experimental cases, *Figures 7* show both maximum relative displacement at the base of the mass (D1-D0) and the acceleration reduction ratio (A1/A0) with passive and semi-active control for each excitation and level of PGA. Plots in these figures for passive operation of the MR damper indicate only the two extremes of the voltage command levels, 'P-off; 0 volt' and 'P-on: 1.0 volt,'. First, it is apparent from these figures that simply attaching the 300 kN MR damper to the structure significantly decreases the relative displacement of the base-isolation system. In addition, the greater the constant command voltage that is sent to the MR damper in a passive mode, the larger the reduction in relative displacement. For semi-active control cases, reductions in the maximum relative displacement are similar in magnitude to the 'P-on' case that uses the maximum command voltage. Since energy supplied to the MR damper can be reduced through use of modulated current, the semi-active control system provides a more efficient means of control than 'P-on' and also reduces the temperature of the MR fluid.

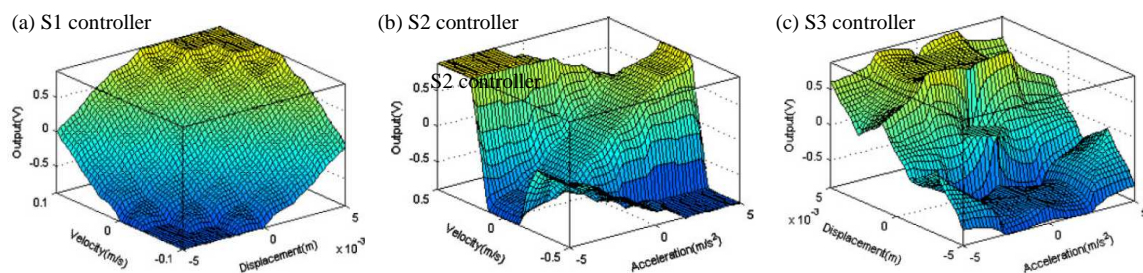


Figure 6. Fuzzy inference system for controller S1, S2 and S3, respectively

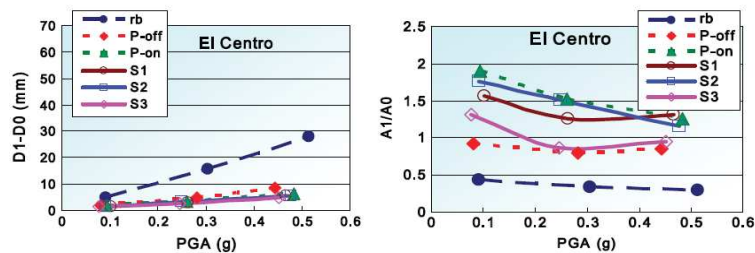


Figure 7. Maximum relative displacement (D1-D0) and acceleration reduction (A1/A0) for different PGA levels of El Centro.

#### 4. CONCLUSIONS

Very small power consumption, high reliability and a fail-safe mechanism make semi-active control one of the more promising approaches for the mitigation of damage due to seismic events in civil engineering structures. This paper presents the lessons learned during the past 10 years on the application of MR-damper to control the building structures through large experimental studies. For experimental studied several control algorithms were also developed which include: H2-LQR, H-infinite, centralized vs. decentralized control, sliding mode control and fuzzy logic control etc. Verification of the control algorithms were conducted through the shaking table test in NCREE using almost full scale structures. The tests include: (1) Displacement control of isolated structures with semi-active control devices, (2) Hybrid base-isolation with magnetorheological damper and fuzzy control, (3) Experimental Verification of Wireless Sensing and Control System for Structural Control Using MR-Dampers, (4) Decentralized Sliding Mode Control of Building Using MR- Dampers, (5) Experimental performance evaluation of an equipment isolation using MR- Dampers. Through these studies the applicability of semi-active control of building structure using MR-dampers had been proven as a powerful control device to mitigate the building responses due to seismic excitations. Based on the experimental studied in NCREE the following lessons were learned:

(1) In the decentralized control design, only local sensor information has been used to generate the control signal that is send to the dampers of each control subsystem. The de-centralized control algorithm can be carried out successfully for a large-scale structural system.

(2) A proper design of control algorithms for the semi-actively controlled isolation system can reduce the peak response acceleration of the equipment without substantially increasing isolator displacement and building structural response.

(3) Fuzzy logic control is effective and easily applied to the semi-active control system. Since energy supplied to the MR damper can be reduced through use of modulated current, another benefit is that the semi-active control system can reduce the temperature of the MR fluid.

## REFERENCES

- [1] Dyke, S. J., Spencer Jr., B. F., Sain, M.K. and Carlson, J. D. (1996). "Modeling and Control of Magnetorheological Dampers for Seismic Response Reduction," *Smart Materials and Structures*, Vol. 5, pp. 565-575.
- [2] Wereley, N. M., Pang L., and Kamath G.M., (1998). "Idealized Hysteresis Modeling of Electrorheological and Magnetorheological Dampers," *Journal of Intelligent Material Systems and Structures*, Vol. 9, pp. 642-649.
- [3] Wen, Y.K., (1976). "Method of Random Vibration of Hysteretic Systems," ASCE, *Journal of Engineering Mechanics Division*, Vol. 102, No. EM2, pp. 249-263.
- [4] Stanway, R., Sproston, J. L., and Stevens, N. G. (1987). "Non-linear modeling of an electro-rheological vibration damper," *Journal of Electrostatics*, Vol. 20, pp. 167-184.
- [5] Chang, C. C. and Zhou, L. (2000). "A recurrent neural network emulator for the inverse dynamics of an MR damper," *Advances in Structural dynamics*, Vol. 1, pp. 365-372.
- [6] Yang, J.N., Akbarpour, A., and Ghaemmaghami, P., (1986). "New optimal control algorithms for structural control," ASCE, *Journal of Engineering Mechanics*, Vol. 113, pp. 1369-1386.
- [7] Limebeer, D.J.N. and Anderson, B.D.O., (1994). "A Nash game approach to Mixed  $H_2/H_\infty$  control," *IEEE Transactions on Automatic Control*, Vol. 39, pp. 69-82.
- [8] Utkin, V.I., *Sliding Modes in Control and Optimization*, Springer-Verlag, New York, 1992.
- [9] Moon, S.J., Bergman, L.A., Voulgaris, P.G., (2003). "Sliding Mode Control of Cable-Stayed Bridge Subjected to Seismic Excitation," ASCE, *Journal of Engineering Mechanics*, Vol. 129, No.1, pp. 71-78.
- [10] Hwang, G. C. and Lin, S. C. (1992). "A stability approach to fuzzy control design for nonlinear systems," *Fuzzy Sets and Systems*, Vol. 48, pp. 279-287.
- [11] Caicedo, J.M., Dyke, S.J., Moon, S.J., Bergman, L.A., Turan, G., and Hague, S., (2003). "Phase II Benchmark control problem for seismic response of cable-stayed bridges," *Journal of structural control*, Vol. 10, pp. 137-168.
- [12] Jansen, L.M. and Dyke, S.J., (2000). "Semi-Active Control Strategies for MR Dampers: A Comparative Study," ASCE, *Journal of Engineering Mechanics*, ASCE, Vol. 126, No. 8, pp. 795-803.
- [13] Jung HJ, Spencer BF, Ni YQ and Lee IW. State-of-the-art of semiactive control systems using mr fluid dampers in civil engineering applications. *Structural Engineering and Mechanics* 2004; **17**(3-4):493-526.
- [14] Lin PY, Roschke P and Loh CH. System identification and real application of a smart magneto-rheological damper. *2005 IEEE International Symposium on Intelligent Control* Limassol, Cyprus, 2005; 989-994.
- [15] C.M. Chang and C. H. Loh, "Seismic Response Control of Cable-Stayed Bridge Using Different Control Strategies," *J. Earthquake Engineering*, Vol.10, Issue 4, July 2006, 481-508.
- [16] C.-H. Loh and C.-M. Chang, "Application of Centralized and Decentralized Control to Building Structure: Analytical Study," *ASCE, J. of Engineering Mechanics*, 2008, 134(11). 970-982.
- [17] J-H. Weng, C.H. Loh, J.N. Yang, "Experimental Study of Damage Detection by Data-Driven Subspace Identification and Finite Element Model Updating," *J. of Structural Engineering*, ASCE, 2009, 135(12).
- [18] K. C. Lu, Loh, C.-H., J. N. Yang, P. Y. Lin, "Decentralized Sliding Mode Control of Building Using MR-Dampers," *Smart Material and Structures*, 17 (5) 2008
- [19] Y.-C. Fan, C. H. Loh, J. N. Yang and P.-Y. Lin, "Experimental performance evaluation of an equipment isolation using MR-Dampers," *Earthquake Eng. & Structural Dynamics*, 38, 285-305, 2009.
- [20] P. Y. Lin, P. N. Roschke, C. H. Loh, "Hybrid base-isolation with magnetorheological damper and fuzzy control", *Structural Control and Health Monitoring* Vol. 14, Issue 3, April 2007, Pages: 384-405.